CASE FILE

NATIONAL ADVISORY COMMITTEE FOR AERONAUTICS

REPORT No. 852

FLIGHT INVESTIGATION AT HIGH SPEEDS OF THE DRAG OF THREE AIRFOILS AND A CIRCULAR CYLINDER REPRESENTING FULL-SCALE PROPELLER SHANKS

By WILLIAM H. BARLOW



AERONAUTIC SYMBOLS

1. FUNDAMENTAL AND DERIVED UNITS

74 O. A.	Symbol	Metric		English		
		Unit	Abbrevia- tion	Unit	Abbrevia- tion	
Length Time Force	l t F	metersecond_ weight of 1 kilogram	m s kg	foot (or mile) second (or hour) weight of 1 pound	ft (or mi) sec (or hr) lb	
Power	P V	horsepower (metric) {kilometers per hour meters per second	kph mps	horsepower miles per hour feet per second	hp mph fps	

2. GENERAL SYMBOLS

Kinematic viscosity

Weight=mg

W

$\begin{array}{llllllllllllllllllllllllllllllllllll$	0	Standard acceleration of gravity=9.80665 m/s ² or 32.1740 ft/sec ²	Stand	Density (mass per unit volume) ard density of dry air, 0.12497 kg-m ⁻⁴ -s ² at 15 ⁶ C
I Moment of inertia= mk^2 . (Indicate axis of radius of gyration k by proper subscript.) 2. AERODYNAMIC SYMBOLS S Area S. Area of wing Gap b Span C Chord Aspect ratio, $\frac{b^3}{S}$ Dynamic pressure, $\frac{1}{2}\rho V^2$ Drag, absolute coefficient $C_{D_0} = \frac{D_0}{qS}$ Profile drag, absolute coefficient $C_{D_p} = \frac{D_t}{qS}$ D, Parasite drag, absolute coefficient $C_{D_p} = \frac{D_t}{qS}$ Profile drag, absolute coefficient $C_{D_p} = \frac{D_t}{qS}$ Prasite drag, absolute coefficient $C_{D_p} = \frac{D_t}{qS}$ Profile drag, absolute coefficient $C_{D_p} = \frac{D_t}{qS}$ Prasite drag, absolute coefficient $C_{D_p} = \frac{D_t}{qS}$ Pright-path angle	112	$\text{Mass} = \frac{n}{a}$	Specif	ic weight of "standard" air 1 2255 kg/m³ or
$ \begin{array}{cccccccccccccccccccccccccccccccccccc$		radius of gyration k by proper subscript.)		
$S_{\bullet \bullet}$ Area of wing i_t Angle of stabilizer setting (relative to thrust line) b Span Q Resultant moment c Chord Ω Resultant angular velocity A Aspect ratio, $\frac{b^3}{S}$ R Reynolds number, $\rho \frac{Vl}{\mu}$ where l is a linear dimentant size of l where l is a linear dimentant size		3. AERODYNAI	MIC SY	MBOLS
S_w Area of wing i_t Angle of stabilizer setting (relative to thrust line) G Gap Q Resultant moment C Chord Ω Resultant angular velocity A Aspect ratio, $\frac{b^3}{S}$ R Reynolds number, $\rho \frac{Vl}{\mu}$ where l is a linear dimension (e.g., for an airfoil of 1.0 ft chord, 100 mph, standard pressure at 15° C, the corresponding Reynolds number is 935,400; or for an airfoil of 1.0 m chord, 100 mps, the corresponding Reynolds number is 6,865,000) D Drag, absolute coefficient $C_D = \frac{D}{qS}$ α Angle of attack Angle of downwash D_{\bullet} Profile drag, absolute coefficient $C_{D_{\bullet}} = \frac{D_{\bullet}}{qS}$ α Angle of attack, infinite aspect ratio Angle of attack, induced D_{\bullet} Induced drag, absolute coefficient $C_{D_{\bullet}} = \frac{D_{\bullet}}{qS}$ α Angle of attack, absolute (measured from zerolift position) D_{\bullet} Parasite drag, absolute coefficient $C_{D_{\bullet}} = \frac{D_{\bullet}}{qS}$ γ Flight-path angle	S	Area	in	Angle of setting of wings (relative to thrust line)
Gap b Span Chord A Aspect ratio, $\frac{b^2}{S}$ R Reynolds number, $\rho \frac{Vl}{\mu}$ where l is a linear dimension (e.g., for an airfoil of 1.0 ft chord, 100 mph, standard pressure at 15° C, the corresponding Reynolds number is 935,400; or for an airfoil of 1.0 m chord, 100 mps, the corresponding Reynolds number is 6,865,000) D Drag, absolute coefficient $C_D = \frac{D}{qS}$ Profile drag, absolute coefficient $C_{D_0} = \frac{D_0}{qS}$ α Angle of attack Angle of attack, infinite aspect ratio Angle of attack, induced Angle of attack, induced Angle of attack, absolute (measured from zerolift position) Parasite drag, absolute coefficient $C_{D_p} = \frac{D_p}{qS}$ Pright-path angle	Su	Area of wing		
cChord Ω Resultant angular velocityAAspect ratio, $\frac{b^3}{S}$ RReynolds number, $\rho \frac{Vl}{\mu}$ where l is a linear dimension (e.g., for an airfoil of 1.0 ft chord, 100 mph, standard pressure at 15° C, the corresponding Reynolds number is 935,400; or for an airfoil of 1.0 m chord, 100 mps, the corresponding Reynolds number is 6,865,000)DDrag, absolute coefficient $C_D = \frac{D}{qS}$ α Angle of attackD_0Profile drag, absolute coefficient $C_{D_0} = \frac{D_0}{qS}$ α Angle of attack, infinite aspect ratioD_tInduced drag, absolute coefficient $C_{D_t} = \frac{D_t}{qS}$ α Angle of attack, inducedD_pParasite drag, absolute coefficient $C_{D_p} = \frac{D_t}{qS}$ α Angle of attack, absolute (measured from zerolift position)D_pParasite drag, absolute coefficient $C_{D_p} = \frac{D_t}{qS}$ α Flight-path angle	G	Gap		line)
A Aspect ratio, $\frac{b^3}{S}$ R Reynolds number, $\rho \frac{Vl}{\mu}$ where l is a linear dimension (e.g., for an airfoil of 1.0 ft chord, 100 mph, standard pressure at 15° C, the corresponding Reynolds number is 935,400; or for an airfoil of 1.0 m chord, 100 mps, the corresponding Reynolds number is 6,865,000) D Drag, absolute coefficient $C_D = \frac{D}{qS}$ D_0 Profile drag, absolute coefficient $C_{D_0} = \frac{D_0}{qS}$ D_1 Induced drag, absolute coefficient $C_{D_1} = \frac{D_1}{qS}$ D_2 Parasite drag, absolute coefficient $C_{D_2} = \frac{D_1}{qS}$ D_3 Parasite drag, absolute coefficient $C_{D_2} = \frac{D_2}{qS}$ D_3 Parasite drag, absolute coefficient D_3 Parasit	6			
True air speed q Dynamic pressure, $\frac{1}{2}\rho V^2$ L Lift, absolute coefficient $C_L = \frac{L}{qS}$ D Drag, absolute coefficient $C_D = \frac{D}{qS}$ D Profile drag, absolute coefficient $C_D = \frac{D}{qS}$ D_t Induced drag, absolute coefficient $C_D = \frac{D}{qS}$ D_t Parasite drag, absolute coefficient $D_D = \frac{D}{qS}$	C		Ω	
True air speed q Dynamic pressure, $\frac{1}{2}\rho V^2$ L Lift, absolute coefficient $C_L = \frac{L}{qS}$ D Drag, absolute coefficient $C_D = \frac{D}{qS}$ D Profile drag, absolute coefficient $C_D = \frac{D}{qS}$ D_t Induced drag, absolute coefficient $C_D = \frac{D}{qS}$ D_t Parasite drag, absolute coefficient $D_D = \frac{D}{qS}$	A	Aspect ratio, $\frac{b^2}{S}$	R	Reynolds number, $\rho \frac{Vl}{u}$ where l is a linear dimen-
The description of the coefficient $C_L = \frac{L}{qS}$ and the coefficient $C_L = \frac{L}{qS}$ and the coefficient $C_L = \frac{L}{qS}$ and the coefficient $C_D = \frac{D}{qS}$ and the coefficient $C_D = \frac{D}{$	V	True air speed		
L Lift, absolute coefficient $C_L = \frac{L}{qS}$ of 1.0 m chord, 100 mps, the corresponding Reynolds number is 6,865,000) D Drag, absolute coefficient $C_D = \frac{D}{qS}$ α Angle of attack Angle of attack, angle of attack, infinite aspect ratio Angle of attack, induced Angle of attack, induced Angle of attack, induced Angle of attack, induced Angle of attack, absolute (measured from zero-lift position) Parasite drag, absolute coefficient $C_{Dp} = \frac{D_p}{qS}$ γ Flight-path angle	q			standard pressure at 15° C, the corresponding
Drag, absolute coefficient $C_D = \frac{D}{qS}$ α Angle of attack Angle of downwash Angle of attack, infinite aspect ratio Angle of attack, infinite aspect ratio Angle of attack, induced Flight-path angle Flight-path angle	L	Lift, absolute coefficient $C_{\mathtt{L}} = \frac{L}{qS}$		of 1.0 m chord, 100 mps, the corresponding
Profile drag, absolute coefficient $C_{D_0} = \frac{D_0}{qS}$ α_0 Angle of attack, infinite aspect ratio Angle of attack, induced Angle of attack, induced Angle of attack, absolute (measured from zero- lift position) Parasite drag, absolute coefficient $C_{D_p} = \frac{D_p}{qS}$ γ Flight-path angle	n	Drag absolute coefficient $C = \frac{D}{C}$	a	
Q_{i} Induced drag, absolute coefficient $C_{D_{i}} = \frac{D_{i}}{qS}$ α_{i} Angle of attack, induced Angle of attack, absolute (measured from zerolift position) Q_{i} Angle of attack, absolute (measured from zerolift position) Q_{i} Flight-path angle of attack, absolute (measured from zerolift position)	D	Diag, absolute coemcient $C_B = qS$	ϵ	
D_t Induced drag, absolute coefficient $C_{D_t} = \frac{D_t}{qS}$ α_a Angle of attack, absolute (measured from zerolift position) D_p Parasite drag, absolute coefficient $C_{Dp} = \frac{D_p}{qS}$ γ Flight-path angle	D.	Profile drag, absolute coefficient $C_D = \frac{D_0}{2}$	α	Angle of attack, infinite aspect ratio
D_p Parasite drag, absolute coefficient $C_{Dp} = \frac{D_p}{qS}$ γ Flight-path angle			α_i	Angle of attack, induced
D_p Parasite drag, absolute coefficient $C_{Dp} = \frac{D_p}{qS}$ γ Flight-path angle	D:	Induced drag, absolute coefficient $C_{D_i} = \frac{D_i}{c^{S}}$	α_a	
C Cross-wind force, absolute coefficient $C_{\sigma} = \frac{C}{qS}$	D_{p}		γ	
	0	Cross-wind force, absolute coefficient $C_{\mathcal{C}} = \frac{C}{qS}$		

REPORT No. 852

FLIGHT INVESTIGATION AT HIGH SPEEDS OF THE DRAG OF THREE AIRFOILS AND A CIRCULAR CYLINDER REPRESENTING FULL-SCALE PROPELLER SHANKS

By WILLIAM H. BARLOW

Langley Memorial Aeronautical Laboratory
Langley Field, Va.

National Advisory Committee for Aeronautics

Headquarters, 1500 New Hampshire Avenue NW, Washington 25, D. C.

Created by act of Congress approved March 3, 1915, for the supervision and direction of the scientific study of the problems of flight (U. S. Code, title 49, sec. 241). Its membership was increased to 15 by act approved March 2, 1929. The members are appointed by the President, and serve as such without compensation.

JEROME C. Hunsaker, Sc. D., Cambridge, Mass., Chairman

Theodore P. Wright, Sc. D., Administrator of Civil Aeronautics, Department of Commerce, Vice Chairman.

Hon. WILLIAM A. M. BURDEN, Assistant Secretary of Commerce.

Vannevar Bush, Sc. D., Chairman, Joint Research and Development Board.

EDWARD U. CONDON, PH. D., Director, National Bureau of Standards.

R. M. Hazen, B. S., Chief Engineer, Allison Division, General Motors Corp.

WILLIAM LITTLEWOOD, M. E., Vice President, Engineering, American Airlines System.

Edward M. Powers, Major General, United States Army, Assistant Chief of Air Staff-4, Army Air Forces, War DepartARTHUR W. RADFORD, Vice Admiral, United States Navy, Deputy Chief of Naval Operations (Air), Navy Department.

ARTHUR E. RAYMOND, M. S., Vice President, Engineering, Douglas Aircraft Co.

Francis W. Reichelderfer, Sc. D., Chief, United States Weather Bureau.

Leslie C. Stevens, Rear Admiral, United States Navy, Bureau of Aeronautics, Navy Department.

Carl Spaatz, General, United States Army, Commanding General, Army Air Forces, War Department.

ALEXANDER WETMORE, Sc. D., Secretary, Smithsonian Institution.

ORVILLE WRIGHT, Sc. D., Dayton, Ohio.

George W. Lewis, Sc. D., Director of Aeronautical Research

JOHN F. VICTORY, LLM., Executive Secretary

Henry J. E. Reid, Sc. D., Engineer-in-charge, Langley Memorial Aeronautical Laboratory, Langley Field, Va.
SMITH J. Defrance, B. S., Engineer-in-charge, Ames Aeronautical Laboratory, Moffett Field, Calif.
Edward R. Sharp, LL. B., Manager, Aircraft Engine Research Laboratory, Cleveland Airport, Cleveland, Ohio
Carlton Kemper, B. S., Executive Engineer, Aircraft Engine Research Laboratory, Cleveland Airport, Cleveland, Ohio

TECHNICAL COMMITTEES

AERODYANMICS
POWER PLANTS FOR AIRCRAFT
AIRCRAFT CONSTPUCTION
OPERATING PROBLEMS

MATERIALS RESEARCH COORDINATION SELF-PROPELLED GUIDED MISSILES SURPLUS AIRCRAFT RESEARCH INDUSTRY CONSULTING COMMITTEE

Coordination of Research Needs of Military and Civil Aviation
Preparation of Research Programs
Allocation of Problems
Prevention of Duplication
Consideration of Inventions

Langley Memorial Aeronautical Laboratory, Langley Field, Va. Ames Aeronautical Laboratory, Moffett Field, Calif.

AIRCRAFT ENGINE RESEARCH LABORATORY, Cleveland Airport, Cleveland, Ohio Conduct, under unified control, for all agencies, of scientific research on the fundamental problems of flight

Office of Aeronautical Intelligence, Washington, D. C.

Collection, classification, compilation, and dissemination of scientific and technical information on aeronautics

REPORT No. 852

FLIGHT INVESTIGATION AT HIGH SPEEDS OF THE DRAG OF THREE AIRFOILS AND A CIRCULAR CYLINDER REPRESENTING FULL-SCALE PROPELLER SHANKS

By WILLIAM H. BARLOW

SUMMARY

Tests have been made at high speeds to determine the drag of models, simulating propeller shanks, in the form of a circular cylinder and three airfoils, the NACA 16–025, the NACA 16–040, and the NACA 16–040 with the rear 25 percent chord cut off. All the models had a maximum thickness of 4½ inches to conform with average propeller-shank dimensions and a span of 20¼ inches. For the tests the models were supported perpendicular to the lower surface of the wing of an XP–51 airplane. A wake-survey rake mounted below the wing directly behind the models was used to determine profile drag at Mach numbers of 0.3 to 0.8 over a small range of angle of attack. The drag of the cylinder was also determined from pressure-distribution and force measurements.

The results of the tests indicated that the drag of the airfoils was lower than that of the cylinder over the Mach number range investigated. The drag reduction obtainable through the use of these airfoil sections in place of a round shank increased with a decrease in airfoil thickness ratio and reached maximum values at a Mach number of 0.63 for the NACA 16–040 airfoils and 0.71 for the NACA 16–025 airfoil.

INTRODUCTION

During recent years the National Advisory Committee for Aeronautics has conducted investigations for the purpose of increasing the efficiency of propellers on airplanes. One of the factors found to increase considerably the losses in propeller efficiency was the high drag of round shanks operating in high-velocity fields. Various methods for reducing shank drag were tried; among these methods was the use of cuffs or propeller shank fairings. Flight-test data from cuffed propellers on streamline bodies are scarce, and the available data were not obtained in any systematic manner so that the relative value of the cuffs tested could not be ascertained. Wind-tunnel tests of thick airfoil sections and cuffed propellers have not been obtained with proper scale, Mach number, and shank relief effects. Because of the scarcity of drag data on thick airfoils operating at high speeds, therefore, data for development and improvement of propeller shanks were considered desirable. A flight-test program was consequently begun at the Langley Laboratory of the NACA in order to determine full-scale relative drag characteristics of

various shanks and shank fairings under conditions approaching those of propeller shanks on a streamline body operating at high forward speeds. A preliminary phase of this program consisted of tests of three thick airfoil models and a circular cylinder; these models were mounted perpendicular to the lower surface of the wing of an XP-51 airplane, which was operated at such speeds as to give local Mach numbers at the model station of from 0.30 to 0.80. At the model station the chordwise pressure gradients due to the wing simulated in some respects the gradients due to a propeller spinner. Tip relief conditions at a propeller shank arising from rapid spanwise decrease in blade thickness were approximated by using models of finite aspect ratio. The results of tests of the three thick airfoil models and the circular cylinder are given in the present paper. A comparison of the speed gains that might be realized by use of these thick airfoils in place of a round propeller shank is presented.

SYMBOLS

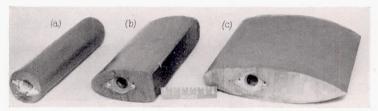
- q dynamic pressure, pounds per square foot
- p_0 free-stream static pressure, pounds per square foot
- Δp local static pressure minus free-stream static pressure, pounds per square foot
- pounds per square root
- d_0 section profile drag of model, pounds per foot of span d section pressure drag of model, pounds per foot of
- D drag of model, pounds
- A frontal area, square feet
- t model thickness, feet
- c_{d_0} section profile-drag coefficient (d_0/qt)
- c_d section pressure-drag coefficient (d/qt)
- C_L airplane lift coefficient
- M₀ flight Mach number
- M effective Mach number at model station

APPARATUS AND METHODS

The propeller-shank sections selected for the tests included a circular cylinder to represent a round shank and two symmetrical airfoils, the NACA 16–025 and the NACA 16–040. The 25-percent-thick airfoil represented a thin shank section and the 40-percent-thick airfoil, a thick shank section. The NACA 16–040 airfoil was also tested with the rear 25 per-

cent chord cut off. A photograph of three of the models tested is presented as figure 1. Geometric characteristics of the models are given in figure 2. All models were of rectangular plan form and had a thickness of $4\frac{1}{2}$ inches to correspond to average shank dimensions. The models had a $20\frac{1}{4}$ -inch span including the rounded tip, which was obtained by rotating the airfoil section 180° about the chord line. The aspect ratios of the models were 9.2, 2.1, 3.4, and 4.5 for the circular cylinder, the NACA 16-025, NACA 16-040, and modified NACA 16-040 airfoils, respectively, and were based on the assumption that the wing acted as a reflection plane. These values of aspect ratio may be high because of a small gap between the model and the wing.

The models were mounted on a rod perpendicular to and extending from the lower surface of the left wing of an XP-51 airplane (fig. 3). The average clearance between the models and the wing surface was $\frac{3}{16}$ inch. (See fig. 4.) Provision was made to rotate the supporting rod in order to obtain a change in angle of attack from -6° to 6° for the



(a) Circular cylinder. (b) Modified NACA 16–040 airfoil. (c) NACA 16–025 airfoil. Figure 1.—Propeller-shank models.

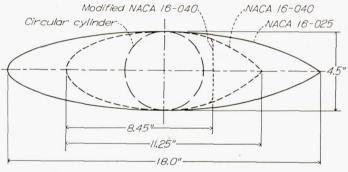


Figure 2.—Geometric characteristics of propeller-shank models. Span of models, 2014 inches, including rounded tip.

airfoils and to rotate the cylinder through 200° for pressuredistribution measurements. The support rod was located at approximately 38 percent of the chord at the 40-percentsemispan station and was about 3 feet outboard of the propeller radius.

A wake-survey rake mounted 29 inches behind the support rod and 9 inches below the wing surface (figs. 4 and 5) provided data for determination of the profile-drag coefficient of the model center section. The distance of the rake behind the trailing edge of each model is shown in figure 5. Direct drag measurements on the cylinder were obtained by mounting the cylinder on a support rod equipped with electric strain gages. Pressure-drag data on the cylinder were obtained from pressure-distribution measurements made by means of two orifices 180° apart at each of six equally spaced spanwise stations (fig. 6). A complete survey at each station was obtained by rotating the cylinder 200° during a test run.

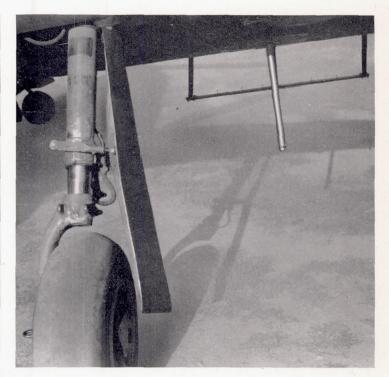


FIGURE 3.—Wake-survey rake and support rod for propeller-shank models mounted on lower surface of wing of XP-51 airplane.



(a) Front view.



Figure 4.—Circular cylinder mounted below lower surface of wing of XP-51 airplane.

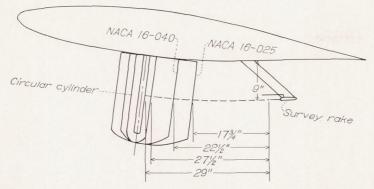


Figure 5.—Location of models and wake-survey rake below lower surface of wing of XP-51 airplane.

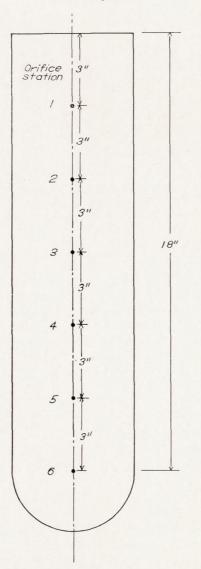


FIGURE 6.—Circular cylinder showing orifice stations.

The local dynamic pressure q and the local Mach number M used in evaluating the data were determined from free-stream total pressure measured with the pitot tube mounted ahead of the airplane wing and from local static pressure measured with static-pressure tubes located on the right wing at the same chordwise and spanwise positions as those at which the models were located on the left wing. These pressure measurements were made simultaneously with

measurements of the drag of the models. In the pressuredistribution tests of the cylinder the static-pressure measurements on the right wing were made with a rake of six static-pressure tubes, with each tube located at a distance below the wing surface corresponding to an orifice location in the cylinder (fig. 6). For the force tests of the cylinder and the wake surveys, the static pressure on the right wing was measured with one static-pressure tube located 9 inches below the wing surface (fig. 7), which corresponds to station 3 in figure 6. The difference between local Mach number at various distances below the wing surface and free-stream Mach number is presented in figure 8 for several flight Mach numbers.

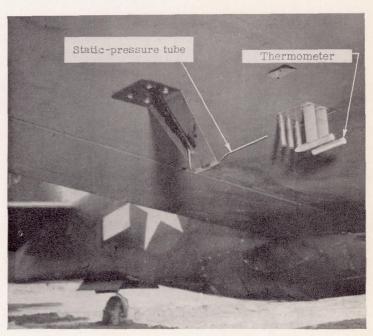


Figure 7.—Static-pressure tube and thermometer mounted below right wing of XP-51 airplane.

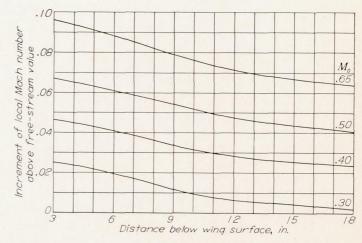


FIGURE 8.—Variation of increment of local Mach number above flight Mach number with distance below right wing surface as determined from static-pressure surveys.

In order to indicate the magnitude of the chordwise variation of static pressure in the test region, the chordwise pressure distributions, as determined from measurements of static pressure on the lower surface of the wing of another XP-51 airplane, are presented in figure 9 for an airplane lift coefficient of about 0.15 and several flight Mach numbers.

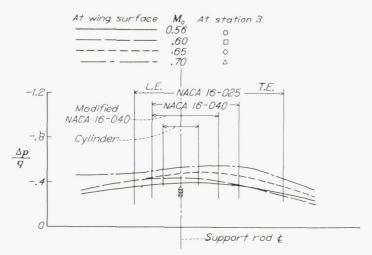


FIGURE 9.—Typical chordwise pressure distributions at wing surface in test region at various flight Mach numbers. Pressure coefficients for station 3 (C_L =0.15) also shown.

Static pressures measured in the present tests at station 3 (9 in. below the wing surface) are included in figure 9. Because of the decrease in induced velocity with distance from the wing surface, the chordwise gradients at station 3 may be somewhat less than those indicated at the wing surface.

The angular position of the models with respect to the airplane longitudinal axis was recorded by a mechanical optical centrol-position recorder. The yaw angle of the airplane was measured by means of a yaw vane mounted on a boom one chord ahead of the right wing near the tip. The angle of attack of the models was determined from the angle of the model and of the airplane. Any difference that might exist between the direction of flow over the wing and the direction of flow in the free stream was not taken into account. Air temperature used in the determination of model Reynolds number was obtained by means of a low-lag thermometer (fig. 7) connected to a recording galvanometer. All instrumentation was standard NACA equipment.

The tests were made at flight Mach numbers from 0.3 to 0.7 in 0.05 intervals. The corresponding range of local Mach number at the test station was 0.3 to 0.8. During each run the flight Mach number, the yaw angle, and the normal acceleration were held constant.

RESULTS AND DISCUSSION

An indication of the extent to which the principal flow conditions about a propeller shank were reproduced in the present model tests may be obtained from an examination of the variation of Mach number with distance from the wing surface (fig. 8), the chordwise variation of static pressure in the test region (fig. 9), and the method used for simulating shank relief. The variation of Mach number with distance from the wing surface indicates that the Mach number decreased by about 0.03 in a distance of about 18 inches, whereas on an actual propeller shank of equivalent length the Mach number (based on the resultant of translational and rotational velocities) would increase by about 0.1. The effect of not reproducing the actual spanwise gradient is not known. The negative chordwise pressure gradients over the

forward part of the test region followed by the positive gradients over the rear part (fig. 9) are similar to the gradients about a spinner on the nose of a typical in-line engine installation. On a propeller the thinner section adjacent to the shank may influence the flow over the shank to some extent. In the present investigation this condition was considered to be simulated, at least approximately, by the use of models of finite aspect ratio.

The variation of the section drag coefficient with Mach number for the cylinder as determined from force-test and pressure-distribution measurements is presented in figure 10. The section pressure-drag coefficient varied over the span of the cylinder, and for tests in which the data are complete no consistent variation is noted. An average minimum section pressure-drag coefficient of 0.5 is found between values of M of 0.425 and 0.475. With further increase in Mach number the section pressure-drag coefficient increased rapidly to a value of about 1.0 at a Mach number of 0.65 and then decreased at still higher Mach numbers. The drag coefficient determined from force tests appeared to be in reasonable agreement with the pressure data.

The drag coefficients of the cylinder determined from force tests, wake surveys, and pressure-distribution tests are compared on the bases of Mach number and Reynolds number in figures 11 and 12, respectively. In general, results of the wake surveys are not in agreement with the results of the force or pressure-distribution tests. Wake-survey results indicated a lower minimum drag coefficient, with drag coefficient increasing rapidly at a Mach number of about 0.425 but increasing to a maximum value of about 1.5 at a value of M of 0.65. This maximum value of drag coefficient is about 50 percent higher than the value obtained by the force and pressure-distribution measurements. No exact explanation for this discrepancy has been ascertained; however, the oscillatory nature of the wake, which is not accounted for in the momentum equations used in reduction of wakesurvey data, may be the cause of this difference. Drag data for the airfoil sections were obtained by the wake-survey

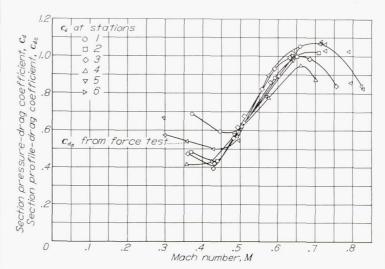


FIGURE 10.—Variation of section drag coefficient with Mach number for the circular cylinder as determined from force-test and pressure-distribution measurements.

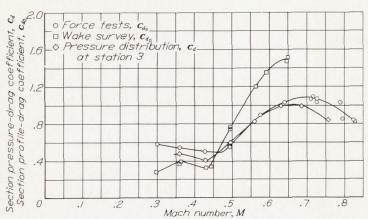


FIGURE 11.—Variation of section drag coefficient with Mach number for the circular cylinder as determined from force tests, wake surveys, and pressure-distribution tests.

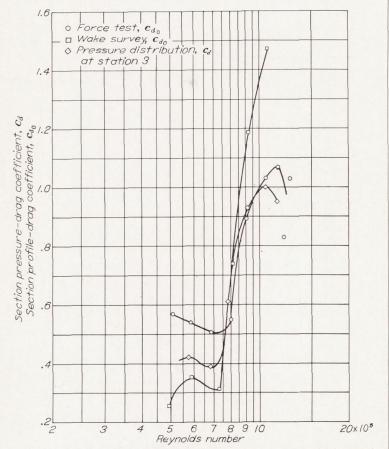
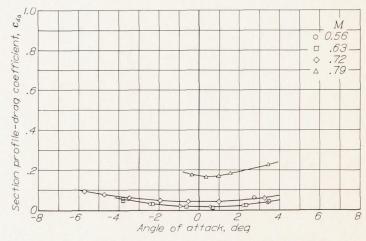


Figure 12.—Variation of section drag coefficient with Reynolds number for the circular cylinder as determined from force tests, wake surveys, and pressure-distribution tests.

method and may therefore be subject to this same type of error. Conditions in the wake of the airfoil at the survey station, however, should approach more closely the conditions assumed in the wake equations than the conditions for the wake of the circular cylinder. If the surveys had been made farther downstream of the models, the effects of wake oscillations might have been reduced and more conservative results obtained. Because of the difficulty of supporting a rake in a more rearward position, however, surveys could not be made farther downstream.

The variation of section profile-drag coefficient with angle of attack for several Mach numbers is presented in figures 13, 14, and 15 for the NACA 16–025, the NACA 16–040, and the modified NACA 16–040 airfoil models, respectively.



 $F_{\rm IGURE~13-Variation~of~section~profile-drag~coefficient~(based~on~thickness)~with~angle~of~attack~at~various~Mach~numbers~for~the~NACA~16-025~airfoil~model.$

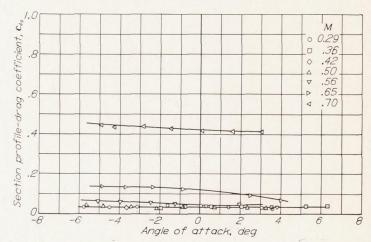


FIGURE 14.—Variation of section profile-drag coefficient (based on thickness) with angle of attack at various Mach numbers for the NACA 16-040 airfoil model.

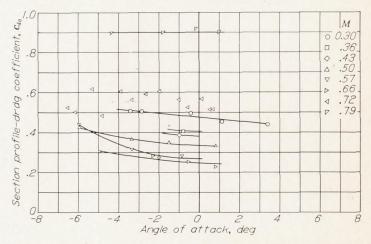


FIGURE 15.—Variation of section profile-drag coefficient (based on thickness) with angle of attack at various Mach numbers for the modified NACA 16-040 airfoil model,

The variation of section profile-drag coefficient with Mach number for zero angle of attack, determined from the data in figures 13 to 15, is presented as figure 16. The section profile-drag coefficient had a minimum value of about 0.02 at Mach numbers up to 0.63 for the NACA 16-025 airfoil model, a minimum value of about 0.04 up to a Mach number of 0.50 for the NACA 16-040 airfoil model, and a minimum value of 0.22 at a Mach number of 0.65 for the modified NACA 16-040 airfoil model. The large values of section profile-drag coefficient, at low Mach numbers, for the modified NACA 16-040 airfoil were probably associated with low Reynolds numbers. The Mach number at which the section profile-drag coefficient began to increase rapidly was 0.75 for the NACA 16-025 airfoil model and 0.60 for the NACA 16-040 airfoil models. At Mach numbers greater than 0.65 the section profile-drag coefficient of the modified NACA 16-040 airfoil model was slightly higher than the corresponding drag coefficient for the NACA 16-040 airfoil model.

The variation of the drag of the cylinder and the airfoil models with Mach number is presented in figure 17 as a plot of D/p_0A against Mach number. Over the range of Mach number tested, the drag of the cylinder was higher than the drag of any of the airfoil models. The drag reduction obtained through use of the airfoils in place of a cylindrical shank increased with decrease in airfoil thickness ratio. A small reduction in drag at low Mach numbers and a large reduction in drag at high Mach numbers can be effected through use of the NACA 16–040 airfoil with the rear 25-percent chord cut off in place of the cylindrical shank. The maximum drag reduction was obtained at a Mach number of 0.63 for the NACA 16–040 airfoils and at a Mach number of 0.71 for the NACA 16–025 airfoil.

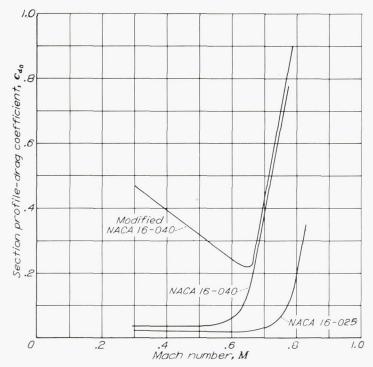


FIGURE 16.—Variation of section profile-drag coefficient (based on thickness) with Mach number for the three airfoil models at zero angle of attack.

On the basis of the results of figure 17 an estimate was made of the increase in speed of a present-day fighter airplane operating at an altitude of 30,000 feet that may be obtained by fairing the exposed round shanks of a four-blade propeller by use of each of the three airfoil sections. The results are presented in figure 18 as the speed increase obtainable by a fairing of 1 inch on each round shank, although, of course, in the actual case more of the propeller shanks would have to be faired and the total increase in speed would therefore be greater than is shown in figure 18. These results are intended primarily to show the relative effectiveness of the various fairings. The maximum increase in speed obtainable by using the NACA 16–040 and the modified NACA 16–040 airfoil sections as fairings was estimated to be 4.0 to 4.5 miles per hour at a true airspeed of 430 miles per

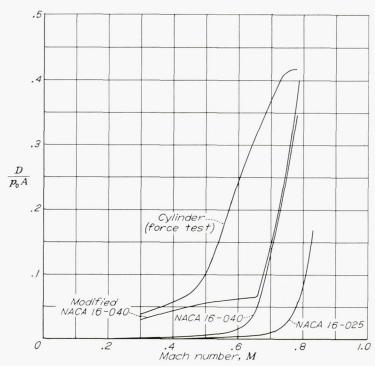


FIGURE 17.—Variation of drag of the circular cylinder and the three airfoil models with Mach number at zero angle of attack.

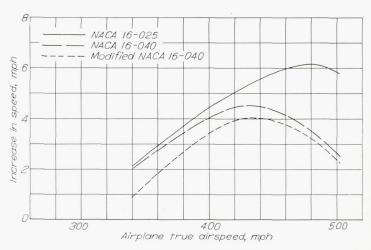


FIGURE 18.—Estimated increase in speed obtainable for a typical fighter airplane with a four-blade propeller by fairing 1 inch of each round shank to an airfoil section. Airplane operating at 30,000 feet.

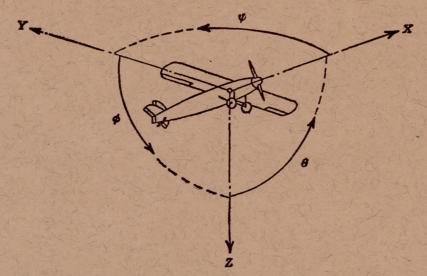
hour. The increase in speed obtainable by using the NACA 16–025 airfoil section was greater over the speed range considered than that obtainable by using the other two airfoil sections and had a maximum value of about 6 miles per hour at a true airspeed of 480 miles per hour.

CONCLUDING REMARKS

The results of tests of models simulating propeller shanks in the form of a cylinder and three airfoils—the NACA 16–025, the NACA 16–040, and a modified NACA 16–040, each having a maximum thickness equal to the cylinder diameter—indicated that the drag of the airfoils was lower than that of

the cylinder over the Mach number range investigated (0.3 to 0.8). The drag reduction obtainable through the use of these airfoil sections in place of a round shank increased with decrease in airfoil thickness ratio and reached maximum values at a Mach number of 0.63 for the NACA 16–040 airfoils and 0.71 for the NACA 16–025 airfoil.

Langley Memorial Aeronautical Laboratory, National Advisory Committee for Aeronautics, Langley Field, Va., June 7, 1946.



Positive directions of axes and angles (forces and moments) are shown by arrows

Axis		Moment about axis			Angle		Velocities		
Designation	Sym- bol		Designation	Sym- bol	Positive direction	Designa- tion	Sym- bol	Linear (compo- nent along axis)	Angular
Longitudinal Lateral Normal	X Y Z	X Y Z	Rolling Pitching Yawing	L M N	$\begin{array}{c} Y \longrightarrow Z \\ Z \longrightarrow X \\ X \longrightarrow Y \end{array}$	Roll Pitch Yaw	φ θ ψ	u v w	p q r

Absolute coefficients of moment

$$C_t = \frac{L}{qbS}$$
 (rolling)

$$C_m = \frac{M}{qcS}$$
 (pitching)

$$C_n = \frac{N}{qbS}$$
 (yawing)

Angle of set of control surface (relative to neutral position), δ. (Indicate surface by proper subscript.)

4. PROPELLER SYMBOLS

r

Geometric pitch

p/D V'Pitch ratio

Inflow velocity

V. Slipstream velocity

Thrust, absolute coefficient $C_T = \frac{T}{\rho n^2 D^4}$

Torque, absolute coefficient $C_Q = \frac{Q}{\rho n^2 D^5}$ Q

Power, absolute coefficient $C_P = \frac{P}{\rho n^3 \overline{D}^6}$

Speed-power coefficient= $\sqrt[5]{\frac{\rho V^5}{Pn^2}}$ C.

Efficiency

Revolutions per second, rps

Effective helix angle= $\tan^{-1}\left(\frac{V}{2\pi rn}\right)$

5. NUMERICAL RELATIONS

1 hp=76.04 kg-m/s=550 ft-lb/sec

1 metric horsepower=0.9863 hp

1 mph=0.4470 mps

1 mps=2.2369 mph

1 lb=0.4536 kg

1 kg=2.2046 lb

1 mi=1,609.35 m=5,280 ft

1 m = 3.2808 ft